

# Low-rate accretion onto single stellar mass black holes

G.M. Beskin<sup>1,2</sup> and S.V. Karpov<sup>1,2</sup>

<sup>1</sup> Special Astrophysical Observatory, Nizhnij Arkhyz, Karachaevo-Cherkesia, 369167, Russia

<sup>2</sup> Isaac Newton Institute of Chile, SAO Branch

Received / Accepted

**Abstract** Magnetic field behaviour in a spherically-symmetric accretion flow for parameters typical of single black holes in the Galaxy is discussed. It is shown that in the majority of Galaxy volume accretion onto single stellar mass black hole will be spherical and have low accretion rate ( $10^{-6} - 10^{-9}$  of Eddington one). A correct analysis of plasma internal energy growth during the fall is performed. Adiabatic heating of collisionless accretion flow due to magnetic adiabatic invariant conservation is 25% more effective than in standard non-magnetized gas case. It is shown that magnetic field line reconnections in discrete current sheets lead to significant nonthermal electron component formation. In a framework of quasi-diffusion acceleration, the "energy-radius" electron distribution is computed and the function describing the shape of synchrotron radiation spectrum is constructed. It is shown that nonthermal electron emission leads to formation of hard (UV, x-ray, up to gamma) highly variable spectral component in addition to the standard (first derived by Shvartsman) synchrotron optical one generated by thermal electrons in magnetic field of accretion flow. Possible applications of these results to single black holes search problem are discussed.

**Key words.** accretion – black hole physics – Galaxy: stellar content – ISM: general – magnetic fields – plasmas – X-rays: general

## 1. Introduction

In spite of the fact that more than 60 years have passed since theoretical prediction of black holes as direct consequences of General Relativity (Oppenheimer & Snyder 1939) in some sense they have not been discovered yet. Really, to identify some object as a black hole, one needs to show that its mass exceeds at least  $3M_{\odot}$ , its size is close to  $r_g = 2GM/c^2$  and it has an event horizon instead of normal surface – the latter is precisely the distinguishing property of black holes which separates them from massive compact objects of finite size in some theories of gravity (Will 1998). However, in fact only two former criteria are used by now for selection of black hole candidates of two types: a) with masses of 5-18  $M_{\odot}$ , in X-ray binaries (see, for example, Greiner et al. 2001); and b) supermassive black holes in galaxy nuclei with masses of  $10^6 - 10^{10} M_{\odot}$  (Shields 1999). Existence of the event horizon in such objects is usually testified by the absence of periodic pulsations of the X-ray emission related to strong regular magnetic fields (black hole "no-hair" theorem) and I type X-ray flares due to thermonuclear bursts of the accreted matter on the surface of a neutron star. At the same time, typical masses of X-ray pulsars and bursters are close to typical neutron star value of 1.4  $M_{\odot}$  while black hole candidates, missing pulsations and X-ray flares, have masses of 5-18

$M_{\odot}$  (Miller et al. 1998). But the absence of event horizon in low-mass objects can't prove its existence at higher-mass ones.

Some of such possible proofs may be the growth of emission redshift and decay near the horizon and the effects of non-diagonal terms of Kerr metric of a rotating black hole. Due to the absence of a theorem similar to Birkhoff one for Schwarzschild metric, a detailed study of the latter effects may be the one possible real proof of black hole nature of the studied object. All stellar mass black holes must be rotating due to angular momentum conservation during the collapse (all stars rotate!). This effect may lead to frozen-in magnetic field regularization and so leads to polarization of its emission. So, the final decision on event horizon detection may be based on the detailed study of physical effects near it – plasma motion, magnetic field growth and reconnections, spectral and temporal features of emission. In order to carry out such analysis we are to be sure that the observed photons are generated near the horizon, which is not the case for contemporary studies of X-ray binaries and galaxy nuclei.

High accretion rates in X-ray binaries and active galactic nuclei lead to the screening of regions close to the event horizon, and the most luminous parts of accretion flow are situated at distances of 10 – 100  $r_g$  (Chakrabarti 1996; Cherepashchuk 2003), where general relativity effects are negligible.

At the same time, single stellar mass black holes, which accrete interstellar medium of low density ( $10^{-2} - 1 \text{ cm}^{-3}$ ), are the ideal case for detection and study of event horizon. Shvartsman (1971) first demonstrated that the emitting halo of the accreted matter forms around such objects and generates optical featureless emission. The majority of such emission comes from the regions near the horizon at  $3 - 5 r_g$ . Spherical accretion onto the single stellar mass black holes has been studied in detail later in the works of several authors (Bisnovatyi-Kogan & Ruzmaikin 1974; Meszaros 1975; Ipser & Price 1977, 1982) and the main conclusions of Shvartsman have been confirmed.

The striking property of the accretion flow onto the single black hole is its inhomogeneity – the clots of plasma act as some kind of probes testing the space-time properties near the horizon. The characteristic timescale of emission variability is  $\tau_v \sim r_g/c \sim 10^{-4} - 10^{-5}$  sec and such short stochastic variability may be considered as a distinctive property of black hole as a smallest possible physical object with given mass. Its parameters – spectra, energetic distribution and light curves carry important information on space-time properties of the horizon (Beskin & Shvartsman 1976). This is in some sense analogous to the so-called “dying pulse trains” – quasi-periodic intensity variations due to rotation of hot spots at internal parts of accretion discs (Sunyaev 1972; Stoeger 1980). However, the latter effect properties are determined by the angular momentum transfer mechanism and disc dynamics mostly, and not by gravitational field of the black hole itself. Also its emission is hardly screened by the accreting plasma and is difficult to detect (Dolan (2000) reports such effect detection at Cyg X-1 at low level of significance).

To complete the picture let’s note two another possibilities for observing the region of the event horizon in X-ray binaries. If the jet of the microquasar is pointed towards us its optical depth is less than unity for distances from a black hole  $r > \frac{2r_g \dot{m}}{\theta^2}$ , where  $\theta$  – the opening angle of jet, and  $\dot{m}$  – the rate of matter ejection in units of Eddington accretion rate. For the typical opening angle  $\theta \sim 0.02$  and  $\dot{m} > 10^{-4}$  we have  $r \sim r_g$ . So-called Ultra-Luminous X-ray sources (Roberts et al. 2002) may be such microquasars. Of course the same situation may occur in active galactic nuclei as well, where black holes have masses of  $10^6 - 10^9 M_\odot$ . At last, in a case of magneto-flaring accretion described by Pustilnik & Shvartsman (1974) accretion flow is a complex of separated plasma clouds, and the region of the event horizon may be seen.

It is necessary to note that general observational appearances of a single stellar-mass black hole at typical interstellar medium density are the same as of other objects without spectral lines – DC-dwarfs and blazars (Shvartsman 1977; Beskin et al. 2000). Consideration of hard spectral bands data (Agol et al. 2002; Chisholm et al. 2002) can’t change the situation dramatically and argue that the object observed is a black hole. As it has been already noted, the only way of black hole identification is detection and detailed study of stochastic emission variations on time scales of  $10^{-6} - 10^{-2}$  sec, related to energy release and evolution of plasma inhomogeneities near the event horizon. This approach is a theoretical base of the observational programme of search for single stellar mass black holes

– MANIA (Multichannel Analysis of Nanosecond Intensity Alterations) (Shvartsman 1977; Beskin et al. 1997). Its main observational method is photometric observations of candidate objects with high time resolution, a special hardware and data analysis methods have been developed for it.

In the framework of this experiment two groups of the objects of  $14^m - 18^m$  with continuous spectra were studied: a) DC-type white dwarfs at distances of  $5 - 50$  pc and proper motions of  $0.02 - 1.8$  arcsec per year (Beskin & Mitronova 1991); b) ROCOSes – radio objects with continuous optical spectra (phenomenologically it is a subclass of blazars) with flat or inverse radio spectra and variability on time scales from days to years (Pustilnik 1977). Note that in contrary to DCs the localization and so the luminosity of ROCOSes are still unknown – no one of them shows proper motion. In Shvartsman et al. (1989a, 1989b), observations of 40 objects were performed on the 6-meter telescope of the Special Astrophysical Observatory of RAS and the upper limits at a level of 20% - 5% on its variability on the timescales of  $10^{-6} - 10$  sec, respectively, were determined. On the basis of variability absence in a sample of 20 most interesting DC dwarfs from Beskin & Mitronova (1991) the upper limits on black holes density of  $5 \cdot 10^{-5} \text{ pc}^{-3}$  in solar neighborhood and  $5 \cdot 10^{-4} M_\odot \text{ pc}^{-3}$  – for hidden mass of Galactic disk (Beskin et al. 2000).

Recently, some evidences appeared that single stellar-mass black holes may be found among the stationary unidentified gamma-ray sources (Gehrels et al. 2002), gravitational lenses causing long-lasting MACHO events (Bennett et al. 2001) and white dwarf – black hole binaries detected by means of self-microlensing flashes (Beskin & Tuntsov 2002). In the latter case mass transfer from the white dwarf is absent and a black hole behaves as a single one. All these cases mean the detection and study of very faint objects of  $19^m - 23^m$ . To solve this problem we’ve created a panoramic photometer-polarimeter of high time resolution able to study faint objects inaccessible with classical aperture photometers (Debur et al. 2003; Plokhhotnichenko et al. 2003).

In the present work we study spherical accretion onto a single stellar-mass black hole at low accretion rates,  $- 10^8 - 10^{13}$  g/s. It corresponds to the range of interstellar medium densities of  $0.002 - 0.1 \text{ cm}^{-3}$  and  $10 M_\odot$  object moving with a velocity of  $20 - 40 \text{ km/s}$  (Bondi & Hoyle 1944). This is true for about 90% of the Galaxy volume (McKee & Ostriker 1977).

Spherical accretion with equipartition of energies, i.e. with roughly equal densities of the magnetic and kinetic energies of plasma has been considered in many papers (Shvartsman 1971; Bisnovatyi-Kogan & Ruzmaikin 1974; Kowalenko & Melia 1999; Ipser & Price 1977, 1982). The uniqueness of our approach is taking into account of a significantly non-thermal nature of electrons (its synchrotron emission determines all observational appearances of a black hole) energy distribution function. It may be roughly considered as a superposition of two components (this approach is known as “hybrid plasma”, see Coppi (1999) and references therein) – thermal electrons and accelerated electron beams, formed in current sheets where magnetic energy is dissipated in a way similar to solar flares (Pustilnik 1978, 1997). The latter process supports the equipartition of energies – the “corner stone” of a modern

picture of spherical accretion (Shvartsman 1971; Bisnovaty-Kogan & Ruzmaikin 1974; Kowalenko & Melia 1999; Ipser & Price 1977, 1982). As a result, the emission of the accretion flow consists of a quasi-stationary "thermal" part with a wide-band spectrum from infrared till ultraviolet, and highly variable flaring nonthermal component. Each such flare is generated due to the motion of the accelerated electron beam in the magnetic field. Its light curve carries information on the magnetic and gravitational field structure near the black hole horizon. Nonthermal luminosity reaches several percents of the total luminosity and may even exceeds at low rates the thermal one, while its spectrum covers spectral bands from optics till hard X-ray. This result leads to possible modifications of search for single black hole strategy.

In §2, main characteristics of accretion onto single black holes in the Galaxy are discussed.

In §3, the electron distribution function in the phase space is built, in §4, the thermal and nonthermal component luminosities are determined, and in §5 the shape of its spectra is studied.

In §6, the temporal behaviour of single electron beam emission is studied and some conclusions on the variability of accretion flow are made.

In §7, the main results of this work are summarized, and in §9, possible directions of future work on this subject are discussed.

## 2. Nature of accretion and basic parameters of the model

Observational appearance of a single black hole is determined by the following factors:

- dynamical characteristics of the black hole itself – its mass and velocity of its motion. Of course, some fine effects may be related also to the metric type, but in this work we'll not consider it and assume that metric is Schwarzschild one (that's generally wrong, as all stars are rotating).
- interstellar medium parameters which determine accretion rate and regime – by its density, temperature and uniformness;
- "average" behaviour of accreting matter, which determines time-averaged luminosity, spectrum and polarization.
- non-stationary processes in the accreting matter, which produce emission parameter variability.

In this paper we'll consider in detail only a), b) and c), and very briefly – d).

### 2.1. Black hole mass and velocity. Interstellar medium and the accretion rate

Contemporary models of the massive star evolution, its dynamics and data on black hole candidates in the X-ray binaries and microlensing events may lead to a conclusion that the most probable mass  $M$  of a single black hole is  $10M_\odot$  (Greiner et al. 2001, Fryer & Kalogera 2001, Agol & Kamionkowski 2002), while its velocity is in 10 – 50 km/s range and the gas capture

cross-section is defined by the Bondi radius  $r_c$  (Bondi & Hoyle 1944):

$$r_c = \frac{2GM}{V^2 + c_s^2}, \quad (1)$$

where  $c_s$  is the sound speed in the interstellar medium.

The interstellar medium consists of at least three components (McKee & Ostriker 1977) – cold ( $T \sim 10^2 K$ ) and dense ( $n \sim 10^2 \text{ cm}^{-3}$ ) neutral hydrogen clouds, hot partly ionized hydrogen ( $n \sim 0.1 - 0.2 \text{ cm}^{-3}$ ,  $T \sim 10^4 K$ ) and fully ionized coronal hydrogen ( $n \sim 0.002 \text{ cm}^{-3}$ ,  $T \sim 10^6 K$ ). So, the black hole motion may be subsonic as well as supersonic – the sound speed changes in the 1.5 – 150 km/s range, correspondingly.

For the black hole moving supersonically in a uniform medium, an accretion rate is determined by behaviour or matter behind the gravitation centre, where tangential gas velocity component vanishes in shock wave and the gas falls towards the black hole in a wide cone (Bondi & Hoyle 1944, Shvartsman 1971, Illarionov & Sunyaev 1975, Font & Ibanez 1998). Note that for typical case of interstellar medium collisionless on scales of the capture radius, a mode of accretion from very thin "tail", where tangential velocity vanishes due to the magnetic field, is possible. Thickness of such a tail may be estimated as

$$\frac{r_{tail}}{r_c} \approx \left( \frac{B_\infty^2 / 8\pi}{\rho V^2 / 2} \right)^{1/2} \approx \frac{c_s}{V}, \quad (2)$$

where  $B_\infty$  is the magnetic field strength at infinity,  $V$  is the black hole velocity and rough equipartition of thermal and magnetic energies in the interstellar medium is taken into account. It is necessary to note that accretion flow is continuous due to interstellar magnetic fields - proton Larmor radius is  $10^7 - 10^8 \text{ cm}$  which is at least  $10^6$  times smaller than  $r_c$ . Interstellar magnetic field in Galaxy ( $10^{-4} - 10^{-5} \text{ G}$ ) is frozen-in. The accretion rate for such a regime is determined by the expression (Bondi & Hoyle 1944)

$$\dot{M} = \frac{4\pi G^2 M^2 \rho}{(V^2 + c_s^2)^{3/2}}, \quad (3)$$

where  $\rho$  is the interstellar medium density.

Using the expression for Eddington accretion rate  $\dot{M}_{edd} = L_{edd} / c^2 = \frac{2\pi m_p c r_g}{\sigma_T} = 1.4 \cdot 10^{18} (M/10M_\odot) \text{ g/s}$ , where  $m_p$  is the proton mass,  $\sigma_T$  – Thompson cross-section, we have a useful normalization, measuring the mass in units of  $10M_\odot$ , density – in  $1 \text{ cm}^{-3}$ , and velocity – in 16 km/s

$$\dot{m} = \dot{M} / \dot{M}_{edd} = 1.3 \cdot 10^{-5} M_{10} n_1 (V^2 + c_s^2)^{-3/2}_{16}. \quad (4)$$

In Fig.1, the dependence of  $\dot{m}$  on  $n$  is shown for various velocities of the black hole motion (the dependence of the sound speed  $c_s$  on the temperature  $T$  due to hydrostatic equilibrium of ISM is also taken into account). Only in the cold clouds the accretion rate may reach Eddington level, but due to relative rareness of such clouds (5% of Galactic volume) this case is improbable. Note however that a black hole may initially be born in such a cloud, and so become a very bright source with

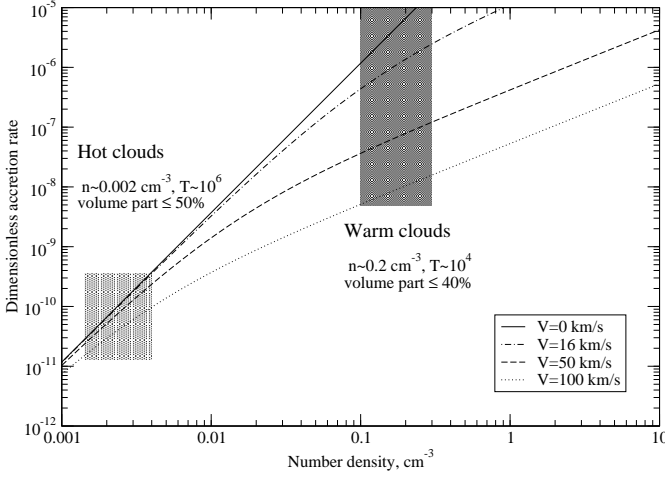


**Figure 1.** Dimensionless accretion rates  $\dot{m} = \dot{M}c^2/L_{edd}$  as a function of interstellar medium density for various black hole velocities.

a luminosity up to  $10^{38} - 10^{40}$  erg/s (and so, be a so-called “ultraluminous” source (Roberts et al. 2002), like that observed in other galaxies). For the hot and warm hydrogen, which volume fraction  $> 50\%$ , the accretion rate will be significantly lower than  $10^{-6} - 10^{-7}$ . Later, we’ll assume exactly such a case as the most typical for single black holes in the Galaxy.

## 2.2. Interstellar medium inhomogeneities role. Spherical or disc-like accretion?

Observational appearances of the accreting black holes depend crucially on the regime of matter flow near the relativistic object. So, in binaries the captured angular momentum of matter is high enough, and a disc-like accretion regime takes place (Shakura & Sunyaev 1973). For the case of accretion from the interstellar medium, however, this problem is more complicated.

In the recent series of papers on the analysis of accretion onto single black holes, it was reasoned that a disc-like regime is realized for such a case also (Fujita et al. 1998; Agol & Kamionowski 2002; Chisholm et al 2002). However, it seems they used overestimated values for the captured angular momentum, and so, let’s review this point in more details.

At first the results of the work Davies & Pringle (1980) should be mentioned. They consider analytically the problem of accretion onto the moving gravitational centre of the non-uniform interstellar medium (inhomogeneities of density as well as of velocity are considered) and show that, in the first order of inhomogeneities, the magnitude accretion rate is still described by Bondi-Hoyle formula (3), and the captured angular momentum is zero.

The latter result may easily be understood by considering a simple model of accretion from the tail in which a traversal velocity component vanishes. This tail, on which the angular momentum is zero by definition, will not, in general, be a straight line, and the capture cross-section will not be a circle, and so, the total captured angular momentum will become zero too. In a more realistic picture, however, the role of gas pressure

is important, the matter accretes in a wide cone, and the total captured angular momentum may be significant, although, as it was shown by numerical simulation results or Sawada et al. (1989), Ruffert (1997, 1999), much smaller than the usually used estimation of Illarionov & Sunyaev (1975):

$$l_m = \frac{1}{4}\beta V_K r_c, \quad (5)$$

(where  $\beta = \frac{\Delta\rho}{\rho}$ ,  $\frac{\Delta V}{V}$  – relative density and velocity variations on  $2r_c$  scale,  $V_K = \sqrt{\frac{V^2 + c_s^2}{2}}$  – Keplerian speed at the capture radius). So, this estimation may be considered as an upper limit which realizes in a very narrow class of objects.

Detailed analysis and numerical simulations leads to more realistic expression for the captured angular momentum (Ruffert 1997, 1999):

$$l \sim 0.1 l_m. \quad (6)$$

For the spherical accretion regime a specific angular momentum of the captured matter must be smaller than that of the black hole last stable orbit, i.e.  $l < \sqrt{3}c r_g$  for Schwarzschild metric. Then

$$\beta < 40 \sqrt{6} \frac{\sqrt{V^2 + c_s^2}}{s}. \quad (7)$$

Due to the characteristic dispersion scale in the interstellar medium being of the order of  $(\Delta V)^2 = 1.1(r/1\text{pc})^{0.76}(\frac{\text{km}}{\text{s}})^2$  (Larson 1981; Falgarone & Phillips 1990), then

$$1.1(\frac{2r_c}{1\text{pc}})^{0.38} < 40\sqrt{3}\frac{V_0^2}{s}, \quad (8)$$

where  $V_0 = \sqrt{V^2 + c_s^2}$ . Finally

$$V_0 > 17M_{10}^{0.138} \text{ km/s}. \quad (9)$$

Therefore nearly for any black hole velocity, interstellar medium turbulent motions can’t prevent realization of spherical accretion regime.<sup>1</sup> Furthermore, density fluctuations can’t prevent it either. For  $\frac{\Delta\rho}{\rho} \sim (\frac{r}{1\text{pc}})^{\frac{11}{6}}$  (Armstrong et al. 1995), it may be easily shown that

$$V_0 > 3.7M_{10}^{0.39} \text{ km/s}. \quad (10)$$

It is clear that even in cold clouds, density fluctuations can’t lead to the disc accretion regime.

## 2.3. Radial structure of the flow

General solution of hydrodynamical problem of accretion onto non-moving gravitating center derived by Bondi (1952) determines radial profiles of various accretion flow parameters as a function of the distance to the black hole, accretion rate and gas adiabatic index. It is important for us that for  $\gamma < 5/3$  (that is always true for interstellar gas) there is a “sonic point” in the flow, by passing which the gas motion becomes supersonic,

<sup>1</sup> As we’ve already noticed, obvious exception is the case of cold clouds where sonic speed is low and at  $v < 16 - 17$  km/s disk may form. We are planning to discuss this case in a separate paper.

and the gas velocity near the gravitating center has an asymptotic behaviour  $v \propto r^{-1/2}$  (and so  $\rho \propto r^{-3/2}$  for density). In the framework of approximate description, we may extrapolate such a behaviour up to the capture radius scale and use it for the whole flow.

In the black hole tail, where the matter flow stops, the thermal, gravitational and magnetic energy densities become nearly equal (since in the collisionless case, the matter is stopped due to the magnetic pressure and plasma oscillations (Illarionov & Sunyaev 1975)). This equipartition of energies (at least magnetic and gravitational ones) preserves in the following infall (so-called Shvartsman equipartition theorem (Shvartsman 1971)), so, we may assume that (Bisnovatyi-Kogan & Ruzmaikin 1974)

$$\frac{B^2}{8\pi} = \frac{1}{2}\rho v^2 = \alpha^2 \frac{GM\rho}{r}, \quad (11)$$

where  $\alpha^2 \approx 1/3$  (which corresponds to equal amounts of gravitational energy transition into kinetic, magnetic and gravitational ones). Therefore, for the parameters of the accretion flow we have

$$v = \alpha c \sqrt{\frac{r_g}{r}} = \alpha c R^{-1/2}, \quad (12)$$

$$\rho = \frac{\dot{M}}{4\pi r^2 v} = \frac{m_p \dot{m}}{2\sigma_T \alpha r_g} R^{-3/2}, \quad (13)$$

$$\frac{B^2}{8\pi} = \frac{1}{2}\rho v^2 = \frac{\alpha m_p c^2 \dot{m}}{4\sigma_T r_g} R^{-5/2}, \quad (14)$$

where the dimensionless values for radius  $R = r/r_g$  and the accretion rate from equation (4) are used. Numerical values of these parameters are

$$n = \frac{\rho}{m_p} = 4.33 \cdot 10^{12} \dot{m}_{-5} M_{10}^{-1} R^{-3/2} \text{ cm}^{-3}, \quad (15)$$

$$B = 8 \cdot 10^4 \dot{m}_{-5}^{1/2} M_{10}^{-1/2} R^{-5/4} \text{ Gauss}. \quad (16)$$

The magnetic field has a quasi-radial (the radial component grows much faster than the tangential one, which is proportional to the square root of distance, magnetic field lines are being stretched) sectorial structure.

The assumption introduced earlier on the equipartition of magnetic, kinetic and gravitational energy requires with necessity the existence of some magnetic flux (and, therefore – magnetic energy) dissipation mechanisms. It was first noted by Shvartsman (1971), their possible observational appearances were discussed by Illarionov and Sunyaev (1975), a model-independent way of estimation of the energy dissipation rate was proposed by Bisnovatyi-Kogan & Ruzmaikin (1974) and from different point of view – by Meszaros (1975), alternative approaches were discussed by Scharlemann (1983) and Kowalenko & Melia (1999).

The dissipation rate of such a mechanism may be estimated as follows (Bisnovatyi-Kogan & Ruzmaikin 1974). Scaling

laws for the magnetic field in a given volume element for the frozen-in field and equipartition are correspondingly

$$\left( \frac{d}{dt} \frac{B^2}{8\pi} \right)_{\text{frozen-in}} = -4 \frac{v}{r} \frac{B^2}{8\pi}, \quad (17)$$

$$\left( \frac{d}{dt} \frac{B^2}{8\pi} \right)_{\text{equipartition}} = -\frac{5}{2} \frac{v}{r} \frac{B^2}{8\pi}, \quad (18)$$

$$\frac{B^2}{8\pi} = \frac{1}{2}\rho v^2 = \alpha^2 \frac{GM\rho}{r}. \quad (19)$$

For the preservation of equipartition state, the power equal to the difference of these expressions must be dissipated in a volume element:

$$\frac{dE}{dV dt} = \frac{3}{2} \frac{v}{r} \frac{B^2}{8\pi}, \quad (20)$$

or the same for a spherical shell

$$\frac{dE}{dR dt} = \frac{3\alpha^2}{4} \frac{\dot{M} c^2}{R^2}, \quad (21)$$

which, by integrating over the whole volume, gives

$$\frac{dE}{dt} = \frac{3}{4} \alpha^2 \dot{M} c^2 = \frac{1}{4} \dot{M} c^2, \quad (22)$$

which means that in the case of equipartition for the spherical flow described earlier, as large as 25% of infalling matter rest energy is released through this dissipation mechanism only. This leads to an additional super-adiabatic heating of the gas (Bisnovatyi-Kogan & Ruzmaikin 1974; Meszaros 1975; Ipser & Price 1977), and unavoidably changes the temperature radial profile and the luminosity of the accretion flow.

#### 2.4. Flaring dissipation of the magnetic field and electron acceleration in the current sheets

It is clear from simple physical reasons that dissipation of the magnetic field means that it is no longer frozen-in, i.e. the mean resistivity becomes much lower and relative motions of the magnetic field and plasma appears (the mean diffusion time becomes comparable to the free-fall one), currents begin to flow and heat the gas. These processes may take place either continuously in turbulent accretion flow as an Ohmic dissipation of magnetic field (Bisnovatyi-Kogan & Ruzmaikin 1974; Bisnovatyi-Kogan & Lovelace 1997) or in compact enough separate regions. In the latter case, the dissipation process has a highly discrete nature (this possibility was noted by Bisnovatyi-Kogan & Lovelace (2000)) of single events of magnetic field line reconnections.

In the present work we consider the latter case. It seems to be more realistic due to the fact that Alfvén velocity which determines the speed of energy exchange between such reconnection region and surrounding plasma is nearly equal to the free-fall velocity at which a high magnetic field gradient region forms. This is analogous to the case of continuous energy supply to the magnetic field inhomogeneities in the solar corona and its flaring (discrete) dissipation and conversion to acceleration of particles and anomalous turbulent heating. This is the

case of formation of turbulent current sheets, which leads to the fast magnetic field line reconnection, avalanche-like growth of energy release (the flare itself) and threshold switch-off of energy dissipation process (Sweet 1969; Petchek 1964; Parker 1979; Spitzer 1954; Syrovatskii 1981). Multi-frequency observations of solar flares evidently support this mechanism. On the other hand, similarity of statistical properties of flaring activity of the Sun (Lu & Hamilton 1991; Lu et al. 1993) and UV Cet stars (Gershberg 1989), X-ray binaries (Kawaguchi & Mineshige 1999) gamma-ray bursts and active galactic nuclei argues in favor of universality of such processes. So, we may assume that the main mechanism providing magnetic energy dissipation in the accretion flow is a reconnection of the magnetic field lines in the current sheets (regions of high magnetic field gradient).

Energy dissipation in the current sheet itself may be considered as a simple Joule heating  $Q = jE = j^2/\sigma$ , where  $j = (c/4\pi) \cdot \text{rot}\mathbf{B} \propto \frac{dB}{a}$  – current density,  $a$  – current sheet thickness,  $\sigma$  – some effective conductivity. It is important that when current reaches some threshold value,  $j_c = en_c c_i$ , where  $n_c$  – electron number density,  $c_i$  – ion sound speed, it becomes to generate strong ion-acoustic turbulence that lowers conductivity by 9-10 orders of magnitude (electrons begin to collide with plasmons and heat it). The analysis of particle acceleration in such current sheet (which may be considered as a superposition of direct electric field acceleration and diffusion - elastic scattering on plasmons) was performed in works of Pustilnik (1978, 1997). In the framework of this model, accelerated particles energy distribution (electrons mostly) naturally appears to be power-law up to energies large enough (Pustilnik 1978) and has a shape

$$f_0(\gamma) = \frac{1}{\Gamma} \left( \frac{\Gamma}{\gamma} \right)^3 e^{-\frac{\Gamma}{\gamma}}, \quad (23)$$

where  $\Gamma$  corresponds to the mean energy of a particle in a beam.

Let's estimate maximal energy electron reaches by acceleration in such current sheet. By using expressions for gas density and magnetic field strength (13),(14) for low accretion rates ( $\dot{m} < 10^{-5}$ ) we deal with, we have for the event horizon  $n \leq 4 \cdot 10^{12}$  and  $B_g \leq 1.7 \cdot 10^5$ . Note, that near  $r_g$  velocities of electrons and plasmons are nearly equal to the speed of light, and so, the maximum current density is  $j_{\max} = enc$ , and the maximum effective field is  $E_{\max} = \frac{enc}{\sigma^*}$ , where  $\sigma^*$  is anomalous resistivity; for our case  $\sigma^* \sim \frac{10^2}{4\pi} \omega_{oe}$ , where  $\omega_{oe}$  – Lengmure frequency ( $\omega_{oe} = 5.65 \cdot 10^4 \cdot n^{1/2}$ ). Therefore, the maximum gamma-factor is

$$\gamma_{\max} \sim \frac{eE_{\max}r_g}{m_e c^2} \sim \frac{e^2 n r_g}{\sigma^* m_e c} \sim \frac{e^2 r_g n^{1/2}}{4.5 \cdot 10^5 m_e c} \sim 10^5. \quad (24)$$

It is very difficult to estimate the fraction  $\xi$  of the dissipated energy carried away by the accelerated particles – electrons during acceleration process generate ion-acoustic and Lengmure plasma oscillations. Also, topology changes in reconnections lead to global matter motions. A study of such processes in the solar flares shows that particles (electrons mostly) carry away from 10% to 50% of energy stored in the magnetic field inhomogeneities (Hudson & Ryan 1995). Let's assume

$\xi = 0.1$  as a reasonable lower limit for further estimations.  $(1 - \xi)$  fraction of the dissipated energy goes into the surrounding plasma heating. In the collisionless case this is due to generation of MHD turbulence in the current sheet. Also, as the speed of plasmons is nearly equal to Alfvén speed, which in turn equals to the free-fall velocity for the equipartition case, the heating is nearly uniform through the whole accretion flow. It is also difficult to determine the motion of the accelerated particle beam. Of course, electrons are flying along the magnetic field lines, tracing its topology. Its motion is local due to relative smallness of Larmor radius in comparison to characteristic scale of the accretion flow, Schwarzschild radius  $r_g$

$$\left( \frac{r_L}{r_g} \right)^2 = \frac{\gamma^2}{\alpha \dot{m}} \frac{m_e}{m_p} \sqrt{\frac{2\sigma_T}{3\pi r_g^2}} \ll 1. \quad (25)$$

For typical single stellar-mass black holes accretion rates, electron-electron and electron-ion energy exchange is highly ineffective (this question has been discussed in details in the framework of advective disk models, see Mahadevan & Quataert (1997) and Bisnovatyi-Kogan & Lovelace (2001)), so we may neglect collisional energy losses for the accelerated particles.

Furthermore, in the case of Maxwellian distribution of the background plasma electrons and moderate mean gamma-factors of the accelerated nonthermal electrons ( $10 - 10^2$  of the mean thermal one), the total electron distribution  $f(\gamma)$  always (for energies above thermal peak) satisfies the inequality  $\frac{df(\gamma)}{d\gamma} < 0$ , and so is stable to the generation of plasmons with wave vectors parallel to the motion direction (Kaplan & Tsytovich 1973). Due to the same reason, all generated instabilities vanish rapidly, the beam is stabilized. However, the induced generation of plasmons with non-collinear wave vectors is possible, this leads to the dissipation of the beam with a characteristic time of  $t_{dis} \sim 10^2 \frac{n_* \gamma_*}{n_* \omega_{oe}}$ , where  $n_*$  is the electron density of the beam (Kaplan, Tsytovich 1973). It is easily seen that  $\frac{t_{dis}}{t_{ff}} \sim r^{-3/4}$ , so, the beam born near  $r_g$  has more chances to survive. Also it is seen that for  $\frac{n}{n_*} > 10^2$  the beam has not enough time to dissipate at the free-fall time scale, so, we may neglect this scattering and thermalization of the beam and consider it as a system of non-interacting electrons in the external magnetic field.

Now let's summarize the model parameters we are going to use below ("minimum model" with minimum reasonable values of particle acceleration coefficients): the fraction of energy released in reconnection carried out by the accelerated electrons is assumed to be  $\xi = 0.1$ , the acceleration parameter (the ratio of the accelerated beam mean energy  $\Gamma$  to the background temperature  $\tau = kT/m_e c^2$ ) is assumed to be constant over the whole accretion flow and equal to  $\Delta = 10$ , and the maximum electron energy in the beam  $\gamma_{\max} = 10^5$  is constant too.

## 2.5. Additional note on the flow structure

The magnetic field dissipation in the current sheet is accompanied by significant dynamical effects, the reconnected magnetic field lines are thrown away through the current sheet butt-ends carrying away the gas that lowers the current sheet density. Due

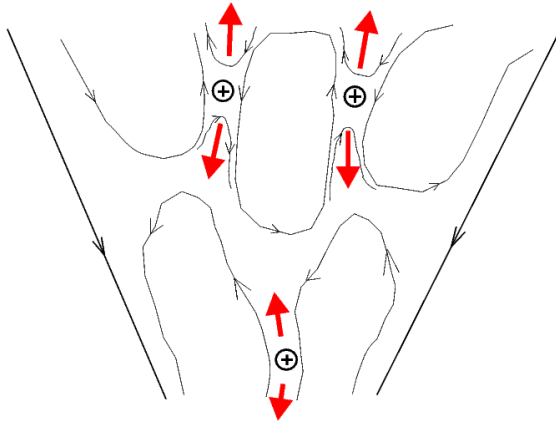


**Figure 2.** A schematic picture of the accretion flow structure. Reconnection regions and ejected plasma flows are shown. The direction of the particles acceleration (current flow) is perpendicular to the viewing plane.

to the radialization of the magnetic field in the accretion flow (Bisnovatyi-Kogan & Ruzmaikin 1974), its gradient is directed tangentially, and so, the current sheets are directed mostly radially. So, the currents and the acceleration of particles are tangential (see Fig. 2). Accretion flow and ejected plasma velocities are close to Alfvén one. Therefore, just after the reconnection, two clouds of plasma with the trapped perpendicular magnetic field lines are flying in opposite directions – one falls supersonically towards the black hole, another nearly stops. Due to its interaction with the surrounding matter, the wave of acceleration is going down, and the one of deceleration – up. As a result, the kinetic energy of the ejected gas is transformed into the accretion flow heating.

It is necessary to note that the results of the solar corona and chromosphere observations (Dere 1996; Innes et al. 1997) show that the reconnection speed is often significantly less than the Alfvén one ( $\approx 0.1 V_A$ ). In such a case the density and temperature fluctuations may not have enough time to vanish, and this may lead to additional variability of the accretion flow.

After the reconnection, the tangential magnetic field lines become radial again, the magnetic field strength and gradients increase and conditions for the development of reconnection appear once more. As it has been already noted, the turbulization of the current sheet (which is the reconnection itself) is a threshold process and begins as the current density exceeds some threshold value. For example, the beam of the accelerated particles ejected from another current sheet, MHD-waves generated there, or ejected plasma may act as such a trigger. So, the accretion flow becomes a complex dynamical system with nonlinear interactions where various fluctuations – of density, velocity, magnetic field strength, particles distribution function – are born and vanish. Local values of the velocity may significantly exceed the sound speed. Let's consider this one in more details. The condition of the energy equipartition of Shvartsman (1971) is an *ansatz* of spherical accretion theory – it determines the fraction of the magnetic energy dissipated

in reconnections and the mean values of the accretion flow parameters and has a form

$$\frac{\rho V^2}{2} = \beta_1^2(r, t) \frac{GM\rho}{r}, \quad \frac{B^2}{8\pi} = \beta_2^2(r, t) \frac{GM\rho}{r}, \quad (26)$$

$$\beta_1^2(r, t) + \beta_2^2(r, t) = 2\alpha^2(r, t). \quad (27)$$

It is clear that physical upper limit for the magnetic energy density is the density of the gravitational energy released (due to energy conservation law), that corresponds to the total stop of matter due to magnetic pressure ( $\beta_1^2 = 0$ ). The dynamics of the accretion flow may be fully described by  $\beta_1$ ,  $\beta_2$  and  $\alpha$  functions. Locally (just after the reconnection) the magnetic field may grow as  $r^{-2}$  and reach maximum value

$$\frac{B^2}{8\pi} \sim 2\alpha^2 \frac{GM\rho}{r}, \quad (28)$$

and then some fraction of it dissipates in the turbulent current sheet.

The magnetic energy dissipation mechanism proposed here is not a unique one. However, it is in a good agreement with the observations of the Sun (Pustilnik 1997). Also, it provides an opportunity for interpretation of the universal energetic spectrum of flares on various objects – from active galactic nuclei till UV-Cet stars in the framework of a single mechanism.

To complete the picture, let's briefly review other models. Fast reconnections leading to particle acceleration were considered by Lazarian & Vishniac (1999, 2000), the role of various instabilities in creation of anomalous resistivity and particles acceleration has been considered by Birk et al. (1999), and processes of particle acceleration in various astrophysical objects – by Bisnovatyi-Kogan & Lovelace (1997, 2000, 2001).

As a general conclusion, it may be noted that the dissipated magnetic energy is converted mostly to acceleration of electrons. In the framework of our paper this means that for analysis of emission processes we may take into account the electron component only.

## 2.6. Note on convection

In the recent works on convection in the accretion flows (numerical simulations of spherical accretion with a magnetic field, and theoretical analysis of the results in Igumenshchev, Narayan (2002), see also works on convection in the advective accretion disks of Narayan et al. (2002) it is noted that in the case of non-adiabatic heating (for example due to magnetic energy dissipation or viscous heating) and negligibly small radiative losses, the specific entropy of matter grows inwards, the accretion flow becomes unstable and a new type solution, a convective one (CDAF – Convection Dominated Accretion Flow, or CDBF – Convection Dominated Bondi Flow), appears. However, the applicability of such the criterion for the collisionless magnetized accretion flow is not straightforward.

In fact, the entropy growth criterion represents that convection starts as soon as the emerging volume element becomes lighter than the surrounding medium (and so continues to emerge). For the stationary accretion flow this is equivalent to the faster growth of gas pressure when the gas element moves

down rather than up. This is clearly correct for the purely gaseous accretion flow due to the existence of non-adiabatic dissipative processes heating the infalling matter. However, in our case the matter is collisionless, and the main contribution to the pressure is due to the magnetic field (the magnetic field is the only agent allowing particles to exchange momentum). But the magnetic field behaviour is inverse in the evaporating matter element the magnetic field changes faster than in the surrounding plasma (in the evaporating element the magnetic field may be treated as perfectly frozen-in, while in the surrounding gas it is, "on the average", dissipated), and so, the evaporating in hydrostatic equilibrium matter element is denser and is forced to immerse back. So, the accretion flow becomes convectively stable.

Also, there exist some other reasons preventing from convection development. Vertical convection is suppressed due to supersonic infall, and a position of the sonic point in the flow is determined by the matter capture mechanism. As it has been noted before, in the case of the supersonic black hole motion, the matter is captured through the "tail" where its perpendicular component vanishes and some fraction of the kinetic energy goes into the thermal and magnetic ones. However, (as the ratio of the thermal to kinetic energy at infinity is

$$\frac{\epsilon_{\text{thermal}}}{\epsilon_{\text{kinetic}}} \approx \left(\frac{a_s}{V}\right)^2 \ll 1 \quad (29)$$

for supersonic motion) it is improbable that the sound speed is higher than the free-fall velocity at the capture radius, and so, we may conclude that the accretion flow is always supersonic and the convection is suppressed.

### 3. Derivation of electron distribution

#### 3.1. Note on adiabatic heating

At low accretion rates considered the gas is fully collisionless, and so particle energy distribution is determined by superposition of three different factors - adiabatic heating, synchrotron cooling and nonthermal heating due to particle acceleration in the current sheets. The former dominates at large distances, and so its precise treatment is very important.

At a level of single particle motion, adiabatic heating of collisionless magnetized gas is due to the conservation of adiabatic invariant (Landau & Lifshitz 1971)

$$I = \frac{3cp_t^2}{2eB} \quad (30)$$

of the charged particle in the magnetic field evolving slowly on a timescale of single Larmor revolution. This basically means the conservation of the phase volume element per particle  $p_t^3 \cdot V = \text{const}$ . Here we neglect the motion parallel to the magnetic field line - only the perpendicular momentum  $p_t$  grows due to compression, while the parallel one  $p_{\parallel}$  is determined mostly by initial conditions.

Note that classical relation between the spatial part of the phase volume and the gas density  $V\rho = \text{const}$ , that is true for normal "gas in a box" of classical thermodynamics, is generally wrong for the magnetized plasma. Exception is the case of

isotropic gas compression with  $B \propto l^{-2} \propto \rho^{2/3}$  - in this case the magnetic field acts as walls of a box, and this leads to usual equations of state  $\epsilon \propto \rho^{5/3}$  for non-relativistic case or  $\epsilon \propto \rho^{4/3}$  - for relativistic one. Here we use the proportionality of particle energy to its perpendicular momentum, that is true for two opposite cases - either for  $p_{\parallel} \propto p_t$  (effective isotropization) or for  $p_{\parallel} \ll p_t$  (collisionless case, only perpendicular momentum increases).

In the case of the accretion flow, however, the gas compression is significantly anisotropic (the matter element is even stretched in the radial direction proportional to  $r^{-1/2}$ ), and the magnetic field itself is not perfectly frozen-in either. So, the relation of the phase volume element spatial part to density becomes

$$\frac{dV}{V} = -3 \frac{dp_t}{p_t} = -\frac{3}{2} \frac{dB}{B} = -\frac{15}{8} \frac{dr}{r} = -\frac{5}{4} \frac{d\rho}{\rho} = -\frac{5}{4} \frac{dn}{n}, \quad (31)$$

where the introduced before radial dependencies (13),(14) of the accretion flow parameters are used.

Note that in contrary to assumptions made in most articles on this subject (Bisnovatyi-Kogan & Ruzmaikin 1974; Shapiro 1973b; Meszaros 1975; Ipser & Price 1977, 1982; Mahadevan & Quataert 1997) we can't use the first law of thermodynamic in the form of "energy per particle"

$$d\left(\frac{\epsilon}{n}\right) = -pd\left(\frac{1}{n}\right) + \dots \quad (32)$$

(the dots here represent the contribution of non-adiabatic processes) to describe the relation of the particle mean energy and the gas density as the density changes don't reflect the behaviour of the particle "walls". A correct form of this equation must take into account the fact that the number of particles  $N$  inside the spatial part of each particle conserving phase volume element is no longer constant

$$d(\epsilon V) = -pdV + \frac{\epsilon}{n}dN + \dots \quad (33)$$

The change of the number of particles using (31) may be expressed as

$$dN = nV \left( \frac{dV}{V} - \frac{d(1/n)}{(1/n)} \right) = -\frac{1}{4}Vdn. \quad (34)$$

For relativistic gas the equation of state has the form  $p = \epsilon/3$ , and so the single particle energy evolution is described by

$$d\left(\frac{\epsilon}{n}\right) = -\frac{5}{12}\epsilon d\left(\frac{1}{n}\right) + \dots, \quad (35)$$

where dots represent possible contribution of non-adiabatic processes per particle (so such particles behave like a gas with specific heat ratio 11/6).

For non-relativistic gas in the similar manner ( $p = \frac{2}{3}\epsilon$ )

$$d\left(\frac{\epsilon}{n}\right) = -\frac{5}{6}\epsilon d\left(\frac{1}{n}\right) + \dots, \quad (36)$$

like the gas with specific heat ratio of 17/12.

Equations (36) and (35) may be rewritten in a form useful for comparison with incorrect expression (32):

$$d\left(\frac{\epsilon}{n}\right) = -\frac{5}{4}pd\left(\frac{1}{n}\right) + \dots. \quad (37)$$



It is easily seen that correct consideration of adiabatic heating makes it 25% more effective than in the case of ideal non-magnetized gas accretion as of Bondi (1952), that has a great influence on luminosity and spectral shape of the accretion flow emission.

### 3.2. Radial temperature distribution

Note that adiabatic heating alone doesn't change the shape of the particle momentum distribution, so initially thermal distribution always stays thermal.

Current sheet spatial scales are usually much smaller than the whole accretion flow one and, therefore, the fraction of the accelerated particles is small, and so, the total (significantly nonthermal) electron distribution may be considered as a superposition of purely thermal one for the background flow particles and purely nonthermal – for the ones accelerated in the current sheets (basically this is the approach known as "hybrid plasma" of Coppi (1999)). Also we assume that for the low accretion rates the non-adiabatic heating and radiative energy losses don't change the shape of thermal component distribution (while changing its mean energy)

$$f(R, \gamma) = f_t(R, \gamma) + \zeta f_{nt}(R, \gamma). \quad (38)$$

Note that this distribution is unnormalized, and only its shape has physical meaning. So, for example, the ratio of nonthermal to thermal electron densities at some radius  $R$  may be expressed as

$$\frac{n_{nt}(R)}{n_t(R)} = \frac{\zeta f_{nt}(R)}{f_t(R)}, \quad (39)$$

where  $f_{nt}(R)$  and  $f_t(R)$  are integrals of the corresponding distribution functions over the where  $\gamma$  range.

Thermal particles distribution function may be written as

$$f_t(R, \gamma) = \frac{\sqrt{R}}{2\tau} \left( \frac{\gamma}{\tau} \right)^2 \exp\left(-\frac{\gamma}{\tau}\right), \quad (40)$$

where a usual dimensionless expression for temperature  $\tau = kT/m_e c^2$  is used. This gives Maxwellian local energy distribution and radial density slope as of  $\rho \propto R^{-3/2}$ .

The temperature distribution  $\tau(R)$  may be determined by solving the energy balance equation taking into account heating due to adiabatic compression and magnetic field dissipation and radiative losses. Note that electrons become relativistic at some large radius  $R_{rel}$ , while protons remain non-relativistic till event horizon (Bisnovatyi-Kogan & Ruzmaikin 1974), and so, its heating rates differ by a factor of 2 (35,36). In the case of ineffective energy exchange (at low accretion rates collisions are very rare, other mechanisms noted in Mahadevan & Quataert (1997) are ineffective either) this could have led to electrons much colder than protons, but due to preferred heating of electrons by non-adiabatic processes (Bisnovatyi-Kogan & Lovelace 2000, 2001) its energies always remain roughly of the same order of magnitude. Of course their gamma-factors will differ by about 40 times, and so the main contribution to the accretion flow radiation is due to electrons. Therefore, only electron temperature is interesting for us.

As it has been noticed before (20), the non-adiabatic heating rate may be expressed as

$$\Phi = (1 - \xi) \frac{dE}{dV dt} = (1 - \xi) \frac{3}{2} \frac{v}{r} \frac{B^2}{8\pi}. \quad (41)$$

The main mechanism of radiative losses at low accretion rates is synchrotron radiation. Its rate may be written as (Lightman & Rybicki 1979)

$$\Lambda_{sync} = \frac{4}{3} \sigma_T c \gamma^2 \frac{B^2}{8\pi} n. \quad (42)$$

For Maxwellian distribution

$$\overline{\gamma^2} = 12 \left( \frac{kT}{m_e c^2} \right)^2 = 12 \tau^2. \quad (43)$$

Taking into account non-adiabatic terms, energy balance equation per particle (36) may be written for non-relativistic region of the flow ( $R > R_{rel}$ ) as

$$\frac{d}{dr} \frac{\epsilon}{n} = -\frac{5}{4} \frac{\epsilon}{nr} + \frac{1}{v} \frac{\Lambda - \Phi}{n}. \quad (44)$$

For non-relativistic electron gas  $\epsilon = \frac{3}{2} nkT$ ; also we may neglect energy losses and rewrite it in variables  $R$  and  $\tau$  as

$$\frac{d\tau}{dR} = -\frac{5}{4} \frac{\tau}{R} - (1 - \xi) \frac{\alpha^2 m_p}{2 m_e} R^{-2}. \quad (45)$$

This gives the value of the radius for that  $\tau = 1$ ,  $R_{rel} \approx 6400$  for  $\xi = 0.1$ , that significantly exceeds  $R_{rel} \approx 1300$  in an ideal gas approximation used by Bisnovatyi-Kogan & Ruzmaikin (1974).

In deeper regions electrons become relativistic, their energy density is  $\epsilon = 3p = 3nkT$ , so for  $R < R_{rel}$  energy balance equation (35) combined with (13), (14) and (4) gives

$$\frac{d\tau}{dR} = -\frac{5}{8} \frac{\tau}{R} - (1 - \xi) \frac{\alpha^2 m_p}{4 m_e} R^{-2} + \frac{4}{3} \frac{m_p}{m_e} \frac{\dot{m} \tau^2}{R^2}. \quad (46)$$

A boundary condition is  $\tau(R_{rel}) = 1$ .

An analytical solution of this equation in general is very difficult, but for the low accretion rates we may neglect the influence of radiative losses and get a solution in a form of

$$\tau(R) = (1 - \xi) \frac{2\alpha^2 m_p}{3 m_e} R^{-1} + \left( 1 - (1 - \xi) \frac{2\alpha^2 m_p}{3 R_{rel} m_e} \right) \left( \frac{R_{rel}}{R} \right)^{5/8}. \quad (47)$$

This expression may be substituted into (40) to get the final expression for thermal electrons distribution.

Applicability of this approximation may be estimated by comparing the timescale of the electron radiative energy losses and the free-fall one near the event horizon

$$\frac{t_{ff}}{t_{rad}} = \frac{\alpha m_p}{3 m_e} \gamma \dot{m} < 1 \quad \text{for} \quad \dot{m} < 10^{-5}, \quad (48)$$

where  $\gamma \approx 100$  is assumed. For higher accretion rates equation (46) may be easily solved numerically.

### 3.3. Distribution function of non-thermal component

Let's build an expression for nonthermal component distribution function. It is clear that we may assume that all electrons are relativistic as only these have significant observational appearances, and electrons are evidently relativistic in most interesting regions near the horizon (much inside relativization radius  $R_{rel} \approx 6000$ ). So, the fraction of the low-energy non-thermal particles is negligible, and nearly all electrons have the "lifetime" not less than the characteristic free-fall time scale (see Sec. 2.4).

So, we may neglect nonthermal particle interaction with electrons and plasmons of the background flow (see discussion in Sec. 2.4) and assume that they evolve due to adiabatic heating and synchrotron energy losses only. Note that this leads to the situation when thermal electron energy grows a bit faster than nonthermal one due to additional heating by plasma oscillations ejected by current sheets.

Energy evolution of single nonthermal electron is described by

$$\frac{d\gamma}{dR} = \frac{1}{3} \frac{m_p}{m_e} \dot{m} \frac{\gamma^2}{R^2} - \frac{5}{8} \frac{\gamma}{R}, \quad (49)$$

where the first term corresponds to synchrotron losses and the second one – to adiabatic heating.

For the initial energy  $\gamma_0$  at  $R_0$  it has a solution

$$\gamma = \frac{\gamma_0}{C_1(R, R_0)\gamma_0 + C_2(R, R_0)} \quad (50)$$

where

$$C_1(R, R_0) = \frac{A}{R} \left( 1 - \left[ \frac{R}{R_0} \right]^{13/8} \right)$$

$$A = \frac{8}{39} \frac{m_p}{m_e} \dot{m}$$

$$C_2(R, R_0) = \left( \frac{R}{R_0} \right)^{5/8}.$$

The nonthermal component at some radius  $R$  consists of non-interacting electron beams generated at all radii  $R_0 > R$ . Evolution of distribution function of each such beam (assuming that ejection process is stationary and initial beam distribution function is  $f_b(R_0, \gamma_0)$ ) is as follows:

$$\begin{aligned} f_b(R, \gamma) &= f_b(R_0, \gamma_0) \frac{d\gamma_0}{d\gamma} \\ &= f_b(R_0, \gamma_0) \frac{(C_1(R, R_0)\gamma_0 + C_2(R, R_0))^2}{C_2(R, R_0)}. \end{aligned} \quad (51)$$

Initial beam distribution has a form (see (23))

$$f_b(R_0, \gamma_0) = \frac{f_b(R_0)}{\Gamma(R_0)} \left( \frac{\Gamma(R_0)}{\gamma_0} \right)^3 \exp \left( -\frac{\Gamma(R_0)}{\gamma_0} \right), \quad (52)$$

where the mean energy

$$\overline{\gamma_0} = \Gamma = \Delta\tau$$

is assumed to be by a fixed factor  $\Delta$  greater than the local thermal component one and  $f_b(R)$  describes radial distribution of

accelerated particles ejection rate  $dN/dt$ . The latter may be computed using (21) as

$$\frac{dN}{dRdt} = \frac{1}{m_e c^2 \Gamma(R)} \frac{\xi dE}{dRdt} = \frac{6\pi\alpha^2 m_p r_g c}{4 m_e \sigma_T R^2 \Gamma(R)} \xi \dot{m}, \quad (53)$$

which gives for the total ejection rate

$$\frac{dN}{dt} = \frac{6\pi\alpha^2 m_p r_g c}{4 m_e \sigma_T} \xi \dot{m} \int_1^\infty \frac{dR}{R^2 \Gamma(R)}, \quad (54)$$

and the radial distribution of particle ejection

$$f_b(R_0) = \frac{a_0}{\Gamma(R_0)R_0^2}, \text{ where } a_0 = \left( \int_1^\infty \frac{dR_0}{\Gamma(R_0)R_0^2} \right)^{-1}. \quad (55)$$

By integrating (51) over all  $R_0 > R$  we may get final expression for nonthermal electron distribution which consists of all beam electrons ejected at greater distances

$$\begin{aligned} f_{nt}(R, \gamma) &= \int_R^\infty \frac{a_0 dR_0}{R_0^2} \frac{\Gamma(R_0)}{\gamma_0^3} \frac{[C_1(R, R_0)\gamma_0 + C_2(R, R_0)]^2}{C_2(R, R_0)} \\ &\quad \times \exp \left( -\frac{\Gamma(R_0)}{\gamma_0} \right). \end{aligned} \quad (56)$$

Now let's determine  $\zeta$  coefficient of the total electron distribution (38). By combining (39) with trivial expressions for energy density ratio

$$\frac{\epsilon_{nt}(R)}{\epsilon_t(R)} = \frac{n_{nt}(R)}{n_t(R)} \frac{\overline{\gamma}_t(R)}{\overline{\gamma}_{nt}(R)} \quad (57)$$

and for energy density of thermal electrons with Maxwellian value  $\overline{\gamma}_t(R) = 3\tau(R)$

$$\epsilon_t = 3m_e c^2 \tau(R) n_t \quad (58)$$

we may get

$$\zeta = \frac{\epsilon_{nt}(R) \sqrt{R}}{m_e c^2 n_t(R)} \left( \int_1^\infty \gamma f_{nt}(R, \gamma) d\gamma \right)^{-1}. \quad (59)$$

A fraction of nonthermal particles is always small, so we may replace here the thermal particle number density  $n_t(r)$  with the total one  $n(R)$ .

Nonthermal electron energy density at  $R$  may be computed by considering elementary spherical shell  $R \div R + \delta R$  and integrating nonthermal energy release in it during its whole back-trace free-fall history

$$\epsilon_{nt}(R) = \frac{1}{4\pi r_g^3 R^2 \delta R} \int_R^\infty \frac{\delta R_0 dR_0}{-\frac{dR_0}{dt}} \left( \frac{\xi dE}{dR_0 dt} \right) \frac{\overline{\gamma}_b(R)}{\Gamma(R_0)}, \quad (60)$$

where the latter multiplicative term corresponds to amplification of the mean gamma-factor of each accelerated electron beam ejected at  $R_0$  in free-fall till  $R$ . This quantity may be written using the results of Appendix A as

$$\frac{\overline{\gamma}_b(R)}{\Gamma(R_0)} = \delta_1 \left( \left( \frac{R}{R_0} \right)^{5/8}, \frac{A\Gamma(R_0)}{R} \left( 1 - \left[ \frac{R}{R_0} \right]^{13/8} \right) \right). \quad (61)$$

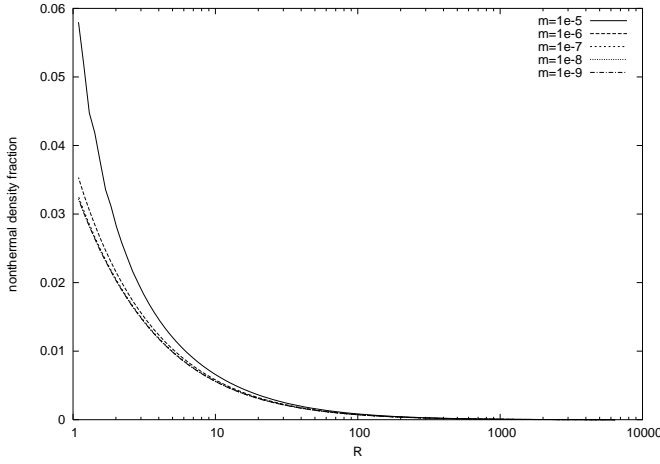


**Figure 3.** Nonthermal electron density fraction  $n_{nt}(R)/n(R)$  for  $M = 10M_\odot$  black hole,  $\xi = 0.1$  and a number of accretion rates.

This one combined with the expression for the local non-thermal energy dissipation rate (21) and with the scaling for the given spherical shell thickness at free-fall  $\delta R_0 \propto R_0^{-1/2}$  leads to the final expression for  $\zeta$  coefficient

$$\zeta = \frac{3}{4} \frac{m_p}{m_e} \xi \alpha^2 \sqrt{R} \left( \int_1^\infty \gamma f_{nt}(R, \gamma) d\gamma \right)^{-1} \times \int_R^\infty \frac{dR_0}{R_0^2} \tilde{\delta}_1 \left( \left( \frac{R}{R_0} \right)^{5/8}, \frac{A\Gamma(R_0)}{R} \left( 1 - \left[ \frac{R}{R_0} \right]^{13/8} \right) \right). \quad (62)$$

A sample fraction of the nonthermal to total densities for different accretion rates is shown in Fig.3 as a function of distance from the black hole. This fraction is small indeed. Fig.4 shows the shapes of thermal and non-thermal distributions for two different distances at small accretion rates.

#### 4. Emission spectrum

The emission spectrum of a single electron for an observer at infinity has the shape (Lightman & Rybicki 1979; Shapiro 1973a)

$$L_\nu = 2\pi \int_{-1}^{\cos \theta^*} j_{\nu'} \frac{1 - \beta^2}{(1 - \beta \cos \theta)^2} d \cos \theta, \quad (63)$$

where relativistic effects of time contraction, gravitational redshift, Doppler effect and the capture of some emission fraction by event horizon are taken into account. The event horizon angular size for free-falling emitter is

$$|\cos \theta^*| = \sqrt{1 - \frac{27}{4R^2} \left( 1 - \frac{1}{R} \right)},$$

where  $\cos \theta^* < 0$  for  $R < 1.5$ . The quantity

$$\beta = \frac{dr}{dt} \frac{1}{1 - r_g/r} = \frac{v/c}{(v^2/c^2 + 1 - r_g/r)^{1/2}}$$

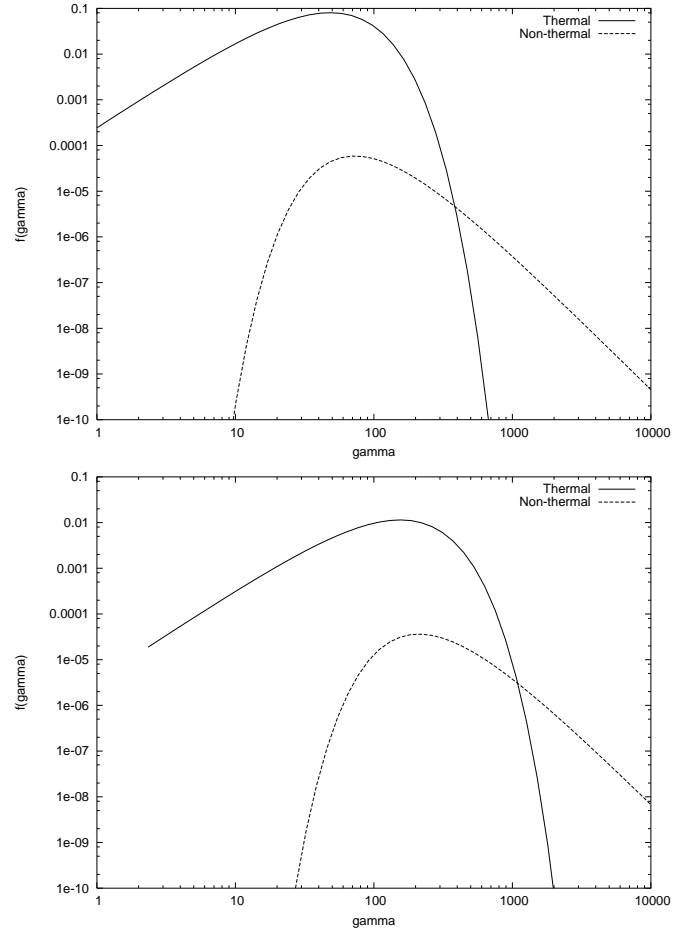


**Figure 4.** Energetic distributions of thermal  $f_t(R, \gamma)$  and non-thermal  $f_{nt}(R, \gamma)$  electron components for distances of  $R = 50r_g$  (first panel) and  $R = 10r_g$  (second panel), respectively.

represents the falling velocity of matter in the distant observer frame, and the frequency shift is given by

$$\nu' = \nu \frac{1 - (v/c) \cos \theta}{\sqrt{(1 - v^2/c^2)(1 - 1/R)}}.$$

By substituting synchrotron emissivity from Lightman & Rybicki (1979) we may get

$$j_\nu = \frac{\sqrt{3}e^3 B \sin \psi}{4\pi m_e c^2} F\left(\frac{\nu'}{\nu_c}\right), \quad (64)$$

$$F(x) = x \int_x^\infty K_{5/3}(\xi) d\xi, \quad (65)$$

$$\nu_c = \frac{3\gamma^2 e B \sin \psi}{4\pi m_e c}. \quad (66)$$

Taking into account the fact that adiabatic compression increases perpendicular electron momentum only (and so we may take  $\sin \psi \approx 1$  for pitch-angle) and convolving with electron distribution (38) the final expression for the accretion flow emission spectrum is

$$L_\nu \propto \int_1^\infty R^{-5/4} dR \int_1^\infty f(R, \gamma) \int_{-1}^{\cos \theta^*} \frac{1 - \beta^2}{1 - \beta \cos \theta} F\left(\frac{\nu'}{\nu_c}\right) d \cos \theta d\gamma. \quad (67)$$

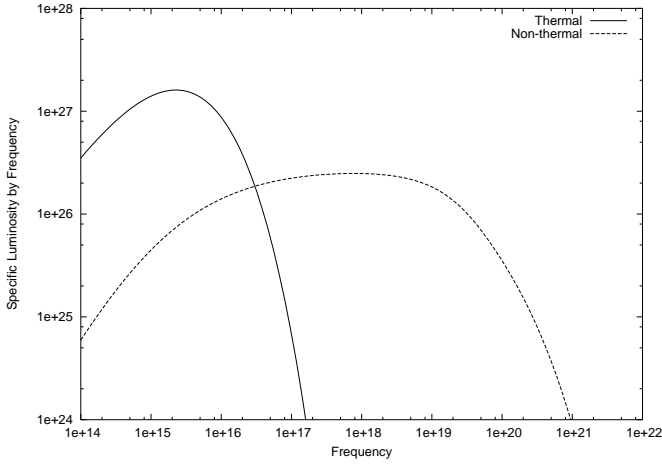


**Figure 5.** Decomposition of a single black hole (with the mass  $10M_{\odot}$ ) emission spectrum into thermal and nonthermal parts. The accretion rate is  $1.4 \cdot 10^{10}$  g/s, which corresponds to  $\dot{m} = 10^{-8}$ .

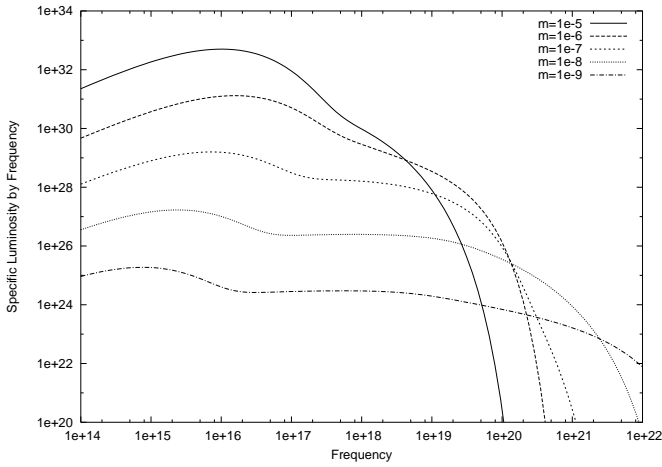


**Figure 6.** Accreting  $10M_{\odot}$  black hole spectra for accretion rates from  $\dot{m} = 10^{-9}$  till  $\dot{m} = 10^{-5}$  ( $\dot{M} = 1.4 \cdot 10^9$  and  $\dot{M} = 1.4 \cdot 10^{13}$  g/s, correspondingly).

Fig. 5 shows a decomposition of the accretion flow spectrum into thermal and nonthermal parts. The fraction of the nonthermal emission is small in optics, but dominates on harder spectral bands. The spectrum becomes flatter with the accretion rate decrease due to increase of electrons radiative losses timescale. High-energy spectral cut-off is determined by radiative energy losses and by the upper limits of the accelerated electron gamma-factor.

## 5. Luminosity

The luminosity of the accretion flow may be computed by integrating expression (67) (Shapiro 1973a; Ipser & Price 1977)

$$L = 8\pi^2 \int_1^{\infty} R^2 dR \int_{-1}^{\cos \theta^*} \int_0^{\infty} j_{\nu'} d\nu' \times \left(1 - \frac{r_g}{r}\right)^{1/2} (1 - \beta^2)^{3/2} (1 - \beta \cos \theta)^{-3} d \cos \theta. \quad (68)$$

Dividing by  $\dot{M}c^2$  and taking into account expression for synchrotron luminosity of a single electron (42), we may get the expression for the efficiency of the thermal component emission

$$\eta_t = 4\dot{m} \int_1^{\infty} \frac{\tau^2}{R^2} K(R) dR, \quad (69)$$

where

$$K(R) = \frac{1}{2} \int_{-1}^{\mu^*} \frac{(1 - 1/R)^{1/2} (1 - \beta^2)^{3/2}}{(1 - \beta x)^3} dx. \quad (70)$$

At low accretion rates ( $\dot{m} \ll 10^{-5}$ ) a reasonably good approximation for this quantity is

$$\eta_t = 4.5 \cdot 10^4 \dot{m}. \quad (71)$$

The efficiency of the nonthermal component emission may be easily estimated from the radial distribution of the dissipated magnetic energy  $dE/dRdt$ , its fraction  $\xi$  carried out by accelerated particles and the evolution of its mean square of gamma-factor during the fall towards the horizon  $\bar{\gamma}_t^2(R)$  as

$$\eta_{nt} = \frac{\xi}{4} \int_1^{\infty} \frac{a_0 dR_0}{\Gamma^2(R_0) R_0^2} \int_1^{R_0} \left( \frac{d\bar{\gamma}}{dR} \right)_{emis} K(R) dR, \quad (72)$$

where the mean radiative energy losses of a single electron are

$$\left( \frac{d\bar{\gamma}}{dR} \right)_{emis} = \frac{1}{3} \frac{m_p}{m_e} \dot{m} \frac{\bar{\gamma}^2}{R^2}. \quad (73)$$

The evolution of the mean square of gamma-factor  $\bar{\gamma}_t^2(R)$  of the beam is given by expression (A.4) derived in Appendix A

So, for the efficiency of the non-thermal component emission we have

$$\eta_{nt} = \frac{a_0 \xi \dot{m}}{12} \int_1^{\infty} \frac{dR_0}{R_0^2} \int_1^{R_0} \frac{dR}{R^2} K(R) \times \mathfrak{F}_2 \left( \left( \frac{R}{R_0} \right)^{5/8}, \frac{A\Gamma(R_0)}{R} \left( 1 - \left[ \frac{R}{R_0} \right]^{13/8} \right) \right). \quad (74)$$

The results of numerical computations according to these formulae may be seen in Fig. 7.

## 6. Properties of flares

Let's discuss some temporal properties of the accretion flow emission. Neglecting the complex spatial structure of the accretion flow we may consider thermal electron component emission  $L_0$  as a constant background which is superimposed with highly variable nonthermal emission component. The variability of the latter is mostly due to discrete nature of particle acceleration in the current sheets. Assuming for simplicity that each non-thermal electron accelerates only once and then free-falls and evolves due to adiabatic heating and radiative losses only, we get for the light curve of a single flare (i.e. a beam

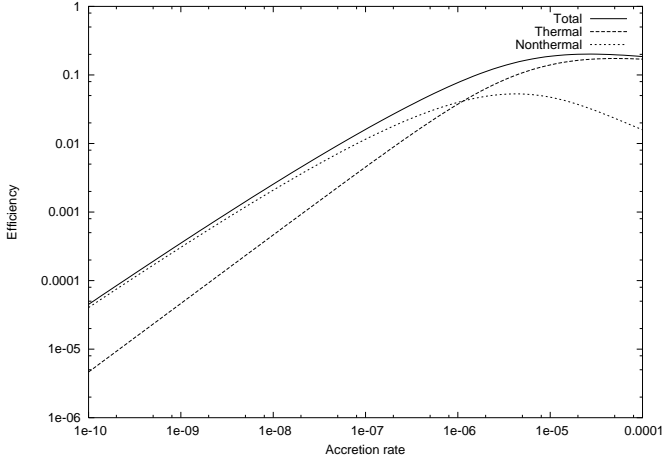


**Figure 7.** Efficiencies of the synchrotron emission of thermal and non-thermal electron components of the accretion flow. The dimensionless accretion rate is  $\dot{m} = \dot{M}c^2/L_{edd}$ .

of  $N$  electrons ejected by a reconnection event at some distance  $R_0$  with distribution function (23) and mean gamma-factor  $\Gamma(R_0) = \Delta\tau(R_0)$  an expression

$$\Delta L = \frac{4}{3}\sigma_T c (\bar{\gamma}_b^2 - 12\tau^2) \frac{B^2}{8\pi} NK(R), \quad (75)$$

where the quantity  $\bar{\gamma}_b^2$  is derived in Appendix A and represents the mean square of gamma-factor of the electron beam ejected at  $R_0$  and free-fallen to  $R$ . The mean square of Maxwellian distribution (40) gamma-factor value of  $12\tau^2$  is also taken into account (we need to subtract this term since each electron must occur in the total luminosity expression only once). The  $K(R)$  coefficient describes relativistic effects of the radiation reduction.

Introducing some effective volume of the current sheet  $V = N/n(R_0)$  and dividing by stationary luminosity of the thermal component  $L_0 = \eta_i \dot{M}c^2$ , we may get

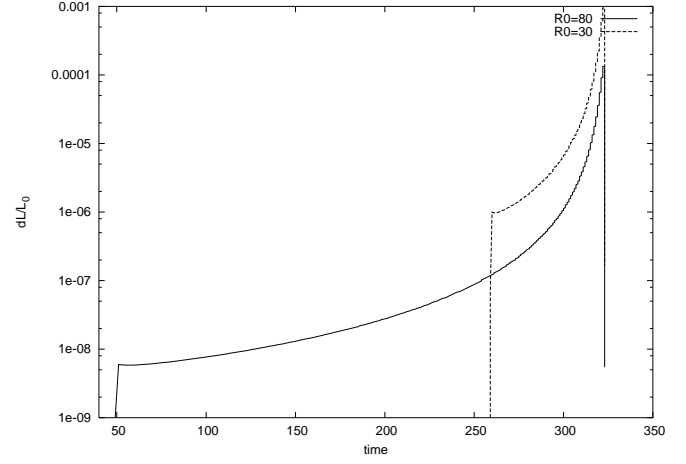
$$\frac{\Delta L}{L_0} = \frac{\dot{m}}{12\pi\eta_i R_0^{3/2}} \left( \frac{V}{r_g^3} \right) \frac{\bar{\gamma}_b^2 - 12\tau^2}{R^{5/2}} K(R). \quad (76)$$

Transition to the light curve may be performed by substituting the dependence of distance on time for the falling gas element as

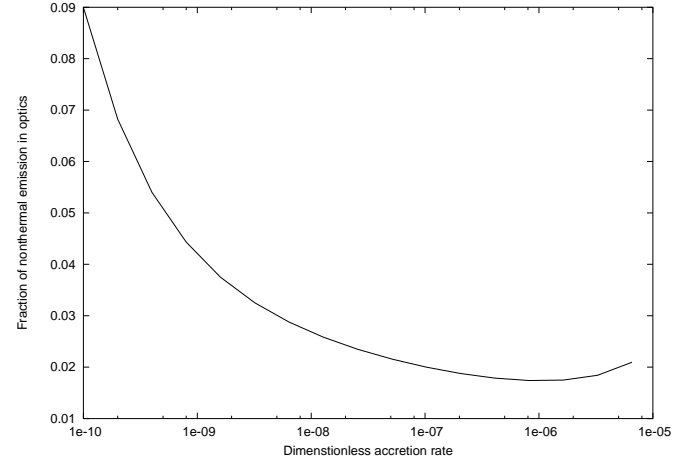
$$R = \left( R_0^{3/2} - \frac{3\alpha}{2} \frac{c}{r_g} t \right)^{2/3}. \quad (77)$$

Fig.8 shows the sample light curves of flares with  $R_0 = 80$  and  $R_0 = 30$  for the accretion rate  $\dot{m} = 10^{-8}$  and the equivalent volume  $V = r_g^3$ . Emission increase is due to relative smallness of radiative losses compared to adiabatic heating. The sharp cutoff is due to relativistic effects of approaching the black hole event horizon.

The fine temporal structure of these flares may be related to the motion of the electron beam in the magnetic field (this motion, as it has been noted before, is finite, electrons don't leave some small volume with the size determined by Larmor radius and magnetic field lines topology). So, if the characteristic size



**Figure 8.** Light curves of single non-thermal flares – beams of accelerated electrons ejected at  $R_0$ . Time is measured in units of  $r_g/c$ , luminosity – in units of total thermal luminosity. Precise shape of the flare front depends on an unknown temporal structure of particle acceleration process.



**Figure 9.** Fraction of nonthermal emission in optics in dependence on dimensionless accretion rate

of the beam (characteristic timescale of particle ejection multiplied by the speed of light) is smaller than that of the magnetic field loops, then we may see the beam emission only when it is pointed right towards us. The timescale of such flares is much shorter than the free-fall one, and they can be detected only in high time resolution observations. On the other hand, their properties reflect the magnetic field structure, and so the task of its search is very important.

Significant amount of nonthermal synchrotron emission also falls into the optical range (see Fig.9). It means that short flares like shown in Fig.8 may be detected in observations with  $1 \mu s$  time resolution at the 6 meter telescope in the framework of MANIA experiment (Beskin et al. 1997).

## 7. Discussion

Let's summarize the results and compare them with those derived in another works.

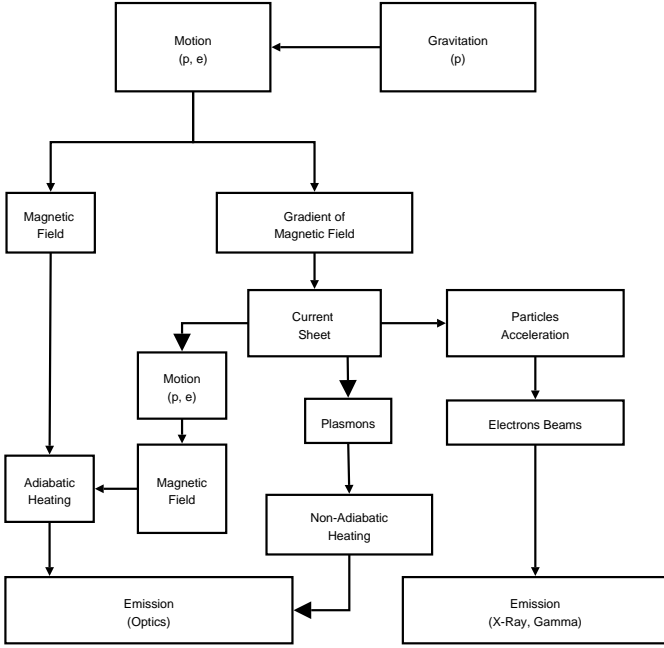


**Figure 10.** Energy conversion in the accretion flow

- The analysis of existing data on possible black hole masses and velocities is performed in comparison with the interstellar medium structure. It is shown that in the majority of cases in the Galaxy ( $> 90\%$ ) the accretion rate  $\dot{m} = \dot{M}c^2/L_{edd}$  can't exceed  $10^{-6} - 10^{-7}$  (see Fig.1). Black holes usually move supersonically (at Mach numbers 2-3). And only in cold clouds of the interstellar hydrogen ( $n \sim 10^2 - 10^5$ ,  $T \sim 10^2$ ) and at low velocities of motion ( $< 10$  km/s) the accretion rates may be high and black hole luminosities may reach  $10^{38} - 10^{40}$  erg/c. For typical interstellar medium inhomogeneity scales and amplitudes  $\Delta\rho/\rho \sim 1$ ,  $\Delta V/V \sim 1$  on 1 pc scale with power-law indices 11/6 and 0.38, respectively the accretion is always (with the exception of the case of a black hole in a dense molecular cloud) spherically-symmetric. This conclusion is in a clear contradiction to the assumptions of Agol & Kamionkowski (2002) work, where the authors assume disk-like accretion onto single stellar-mass black holes.
- The accreting plasma is initially collisionless, and it remains the same till the event horizon. Electron-electron and electron-ion free path  $\lambda \sim 2.4 \cdot 10^3 T^2 n^{-1}$  even at the capture radius is as high as  $\sim 10^{12}$  cm. And only the magnetic fields trapped in plasma (protons Larmor radius at  $r_g$  is 10 cm) make it possible to consider the problem as a quasi-hydrodynamical one, it is only due to magnetic field the particle's momentum doesn't conserve, allowing particles to fall towards the black hole. So, the accretion rate is  $(c/V_0)^2 \sim 10^9$  times higher than in the case of accretion of dust-like matter described in Shapiro & Teukolsky (1973c). In addition to that, the magnetic field effectively "traps" particles in a "box" of a variable size, which allows us to consider its adiabatic heating during the fall; a correct treatment of such process shows that for the magnetized plasma such heating is 25% more effective than

for the ideal gas. Therefore, the plasma temperature in the accretion flow grows much faster, electrons become relativistic earlier ( $R_{rel} \approx 6000$  in contrast to  $R_{rel} \approx 1300$  in the work of Bisnovatyi-Kogan & Ruzmaikin (1974) and  $R_{rel} \approx 200$  in Ipser & Price (1982)), and the accretion flow is much hotter than that predicted in the earlier works of Bisnovatyi-Kogan & Ruzmaikin (1974), Shapiro (1973b), Ipser & Price (1977, 1982).

- The basis of our analysis is the assumption of the energy equipartition in the accretion flow of Shvartsman (1971). Currently, there are no successful attempts to build the magnetized plasma accretion theory without this assumption – the work of Kowalenko & Melia (1999) has led to unphysical results, while Scharlemann (1983) seems to have some mathematical errors in computing the back-reaction of the magnetic field on the matter. The straight consequence of this assumption is the necessity of exceeding magnetic energy dissipation (20). We considered conversion of the magnetic energy in the turbulent current sheets (Pustilnik 1997) as a mechanism providing such dissipation. At the same time, various modes of plasma oscillations are generated (ion-acoustic and Langmuir plasmons mostly), magnetic field lines reconnect and are ejected with plasma from the current sheet and electrons are accelerated. The latter effect is very important for the observational appearances of the whole accretion flow. The beams of the accelerated electrons emit its energy due to motion in the magnetic field and generate an additional (in respect to synchrotron emission of thermal particles) nonthermal component. These electrons have power-law energy distribution and its emission spectrum is flat up to gamma band (Figs.5 and 6). An important property of the nonthermal emission is its flaring nature – the electron ejection process is discrete, typical light curves of single beams are shown in Fig. 8. The light curve of each such flare has a stage of fast intensity increase and sharp cut-off, its shape reflects the properties of the magnetic field and space-time near the horizon.
- The presence of a discrete set of the current sheets complicates significantly the structure of the accretion flow (see Sec. 2.3). It Fig.10 the sketch of energy conversion and plasma internal dynamics is presented. The next possible step in the study of this problem implies the transition from the use of the averaged values (see Sec.2) to consideration of real varying in time and space velocity, density and magnetic field strength.
- In essence, the accretion flow is a complex dynamical system with nonlinear feedbacks. The latter are ensured by the plasma oscillations generated in each reconnection event, beams of the accelerated electrons and clouds of the magnetized plasma ejected from current sheets. All these agents may act as triggers for already "prepared" inhomogeneities which turn on magnetic energy dissipation processes. This situation seems to be similar to the Solar one determining its flaring activity, and also to the case of UV Cet stars and maybe accretion disks of X-ray binaries and active galactic nuclei. All these non-stationary processes are characterized by power-law scalings of flare energies with similar slopes of 1.5-2 at a very wide range

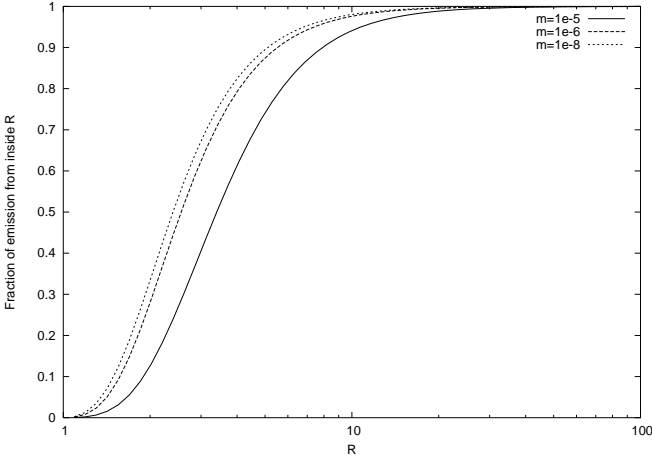


**Figure 11.** Fraction of thermal synchrotron emission that comes from inside given radius  $R$

of energies – from  $10^{23}$  erg/s for the Sun till  $10^{45}$  erg/s for quasars. Universality of these processes may be interpreted in the framework of fractal approach as it has been made by Bak, Tang & Wiesenfeld (1987), Lu & Hamilton (1991), Lu et al. (1993), Anastasiadis, Vlahos & Georgoulis (citeanastasiadis), Kawaguchi & Mineshige (1999), Pustilnik (1997). This means the realization (at least in active phases) of some collective state, sometimes called as “self-organized criticality” (Bak, Tang & Wiesenfeld 1987)), which is characterized by the same behaviour of the parameters on all scales. These are percolation processes. There are evidences that the accretion flow is in this state, and so its observational appearances (at least those related to non-stationary processes) may be predicted and interpreted in the framework of this approach. Initial steps in this direction have been done by Beskin & Karpov (2002), but, of course, it needs to be studied much deeper and wider.

## 8. Conclusions

During several last years the number of works dealing with single stellar-mass black holes has significantly increased. It is necessary to point to purely theoretical ones (Punsly 1998a, 1998b; Gruzinov & Quataert 1999; Abramowicz et al. 2002) as well as discussions of ways of their observational detection (Heckler & Colb 1996; Fujita et al. 1998; Beskin et al. 2000; Agol & Kamionkowski 2002; Chisholm et al. 2002). Great importance of experiments in strong gravitational fields has been recently noted by Damour (1998).

In this work we tried to concretize some possible physical properties of plasma accreted onto the black hole while staying inside classical paradigm of equipartition assumption of Shvartsman (1971). Assumption on the discrete nature of the magnetic energy dissipation processes in current sheets allows us to clarify the shape of synchrotron spectrum of the accretion flow. Hard highly non-stationary nonthermal spectral component appears as an emission of accelerated particles. The

beams accelerated in the current sheets can generate very short flares bringing information about event horizon neighbourhood (Fig.8). On the other hand it is clear from Fig.11 that at low accretion rates significant amount of thermal synchrotron radiation is generated inside  $3r_g$  - it means that behaviour of this component will reflect properties of space-time in strong gravitational fields too.

It is clear that search for black holes strategy may be corrected in accordance with such results. Optical high-time resolution studies of X-ray sources may be very important. Single black holes may be contained inside the known stationary gamma sources (Gehrels et al. 2000) as well as objects causing long microlensing events (Paczynski 1991). So it is very important to look for X-ray emission as well as for fast optical variability of these objects. Sample observations based on such strategy have been performed in the Special Astrophysical Observatory of RAS in the framework of MANIA experiment in the 2003 summer (Beskin et al.2004).

It is pertinent to note once more that detection of the event horizon signatures can't be a result of statistical studies. In any case, a detailed study of each object is needed to detect its specific appearances.

*Acknowledgements.* This work has been supported by Russian Foundation for Basic Research (grant No. 01-02-17857) and by the grant in the frame of CNR (Italy) – RAS (Russia) agreement on scientific collaboration. We also glad to thank T.Tupolova for help in manuscript preparation.

## Appendix A: Moments of single accelerated beam energy distribution

For the case of the electron beam ejected from the current sheet at some radius  $R_0$  and free-falling till  $R$  non-interacting with the background particles and beams ejected below the moments of the energy distribution may be written using (50) as

$$\bar{\gamma}_b(R) = \left( \int_1^\infty f(R_0, \gamma_0) d\gamma_0 \right)^{-1} \int_1^\infty \frac{f(R_0, \gamma_0) \gamma_0 d\gamma_0}{C_1(R, R_0) \gamma_0 + C_2(R, R_0)} \quad (\text{A.1})$$

$$\bar{\gamma}_b^2(R) = \left( \int_1^\infty f(R_0, \gamma_0) d\gamma_0 \right)^{-1} \int_1^\infty \frac{f(R_0, \gamma_0) \gamma_0^2 d\gamma_0}{C_1(R, R_0) \gamma_0 + C_2(R, R_0)} \quad (\text{A.2})$$

For the initial distribution of the form (23) this may be evaluated as

$$\bar{\gamma}_b(R) = \Gamma(R_0) \mathfrak{F}_1 \left( \sqrt{\frac{R}{R_0}}, \frac{A\Gamma(R_0)}{R} \left( 1 - \left[ \frac{R}{R_0} \right]^{3/2} \right) \right) \quad (\text{A.3})$$

$$\bar{\gamma}_b^2(R) = \Gamma^2(R_0) \mathfrak{F}_2 \left( \sqrt{\frac{R}{R_0}}, \frac{A\Gamma(R_0)}{R} \left( 1 - \left[ \frac{R}{R_0} \right]^{3/2} \right) \right) \quad (\text{A.4})$$

where new functions

$$\begin{aligned} \mathfrak{F}_1(A, B) &= \int_0^\infty \frac{x e^{-x} dx}{Ax+B} \\ &= \frac{1}{A^2} \left( A - B \cdot \exp\left(\frac{B}{A}\right) \text{Ei}_1\left(\frac{B}{A}\right) \right) \end{aligned} \quad (\text{A.5})$$

$$\begin{aligned}\mathfrak{F}_2(A, B) &= \int_0^{\infty} \frac{x e^{-x} dx}{(Ax+B)^2} \\ &= \frac{1}{A^2} \left( -A + (1+B) \cdot \exp\left(\frac{B}{A}\right) \text{Ei}_1\left(\frac{B}{A}\right) \right)\end{aligned}\quad (\text{A.6})$$

are introduced and an expression for the integral exponent

$$\text{Ei}_n(x) = \int_1^{\infty} \frac{e^{-\xi x} d\xi}{\xi^n}. \quad (\text{A.7})$$

is used.

## References

- Abramowicz, M.A., Kluzniak, W., & Lasota, J.P. 2002, *astro-ph/0207270*
- Agol, E., Kamionkowski, M., Koopmans, V.E., & Blandford, R.D. 2002, *ApJ*, 576, 131
- Agol, E., & Kamionkowski, M. 2002, *MNRAS*, 334, 553
- Anastasiadis, A., Vlahos, L., & Georgoulis, M.K. 1997, *ApJ*, 489, 367
- Armstrong, J.W., Rickett, B.J., Spangler, S.R., 1995 *ApJ*, 443, 209
- Bak, P., Tang, C., & Weisenfeld, K. 1987, *Phys. Rev. Lett.*, 59, 381
- Bennett, D.P., Becker, A.C., Calitz, C.C. et al. 2001, *astro-ph/0109467*
- Beskin, G.M., Shvartsman, V.F. 1976, in "Relativistic Astrophysics, Cosmology and Gravitational Experiment", M, 9
- Beskin, G.M., & Mitronova, S.N. 1991, *Bulletin of the SAO RAS*, 32, 33
- Beskin, G.M., Komarova, V.N., Neizvestny, S.I. et al. 1997, *ExA*, 7, 413
- Beskin, G.M., Shearer, A., Golden, A. et al. 2000, In: "Texas in Paris", CD-ROM 12/06
- Beskin, G.M., & Karpov, S.V. 2002a, *Gravitation and Cosmology Suppl. Ser.*, 8, 182
- Beskin, G.M., & Tuntsov, A.V. 2002b, *A&A*, 394, 489
- Beskin, G.M., Karpov, G.M., Plokhotnichenko, V.L., et al. 2004, in preparation
- Birk, G.T., Lesch, H., Schopper, R., & Wiechen, H. 1999, *Aph*, 11, 63
- Bisnovatyi-Kogan, G.S., & Ruzmaikin, A.A. 1974, *Ap&SS* 28, 45
- Bisnovatyi-Kogan, G.S., & Lovelace, R.V.E. 1997, *ApJ*, 486, L43
- Bisnovatyi-Kogan, G.S., & Lovelace, R.V.E. 2000, *ApJ*, 529, 978
- Bisnovatyi-Kogan, G.S., & Lovelace, R.V.E. 2001, *NewAR*, 45, 663
- Bondi, H., & Hoyle, F. 1944, *MNRAS*, 104, 273
- Bondi, H. 1952, *MNRAS*, 112, 195
- Chakrabarti, S.K. 1996, *Phys. Rep.*, 266, 229
- Cherepashchuk, A.M., *Usp.Fiz.Nauk*, 173, 345
- Chisholm, J.R., Dodelson, S., & Kolb, E.W. 2003, *ApJ*, 596, 437
- Coppi, P.S. 1999, *astro-ph/9903158*
- Damour, T. 1998, 19th Texas Symposium on Relativistic Astrophysics and Cosmology proceedings, 371
- Davies, R.E., & Pringle, J.E. 1980, *MNRAS*, 191, 599
- Debur, V., Arkhipova, T., Beskin, G., et al. 2003, *Nuclear Instruments and Methods in Physics A*, 513, 127
- Dere, K.P. 1996, *ApJ*, 472, 864
- Dolan, J.F. 2000, *A&AS*, 197, 118
- Falgarone, E., & Phillips, T.G. 1990, *ApJ*, 359, 344
- Font, J.A., Ibanez, J.M. 1998, *ApJ*, 494, 297
- Fryer, C.L., & Kalogera, V. 2001, *ApJ*, 554, 548
- Fujita, Y., Inoue, S., Nakamura, T., et al. 1998, *ApJ*, 495, 85
- Gehrels, N., Macomb, D.J., Bertsch, D.L., et al. 2000, *Nature*, 404, 363
- Gershberg, R.E. 1989, *Memorie Soc.Ast.Ital.*, 59, 1
- Greiner, J., Cuby, J.-G., & Mc Caughrean, M.J. 2001, *Nature*, 414, 522
- Gruzinov, A., & Quataert, E. 1999, *ApJ*, 520, 248
- Heckler, A.F., & Colb, E.W. 1996, *ApJ*, 472, 85
- Hoyle, F., & Lyttleton, R.A. 1939, *Proc. Camb. Phil. Soc.*, 35, 592
- Hudson, Y., & Ryan, J. 1995, *ARA&A*, 33, 239
- Igumenshchev, I., & Narayan, R. 2002, *ApJ*, 566, 137
- Illarionov, A.F., & Sunyaev, R.A. 1975, *A&A*, 39, 185
- Innes, D.E., Inhester, B., Axford, W.L., & Wilhelm, K. 1997, *Nature*, 386, 811
- Ipser, J.R., & Price, R.H. 1977, *ApJ*, 216, 578
- Ipser, J.R., & Price, R.H. 1982, *ApJ*, 255, 654
- Kaplan, S.A., & Tsytovich, V.N. 1973, "Plasma Astrophysics", International Series of Monographs in Natural Philosophy, Oxford: Pergamon Press
- Kawaguchi, T., & Mineshige, S. 1999, *PASP*, 52, L1
- Kowalenko, V., & Melia, F. 1999, *MNRAS*, 310, 1053
- Landau, L.D., & Lifshitz, E.M. 1971, "Classical theory of fields", Course of theoretical physics – Pergamon International Library of Science, Technology, Engineering and Social Studies, Oxford: Pergamon Press
- Larson, R.B., 1981, *MNRAS*, 194, 809
- Lazarian, A., & Vishniac, E.T. 1999, *ApJ*, 517, 700
- Lazarian, A., & Vishniac, E.T. 2000, *astro-ph/0002067*
- Lightman, A.P., & Rybicki, G.B. 1979, "Radiative Processes in Astrophysics:
- Lu, E.T., & Hamilton, R.J. 1991, *ApJ*, 380, 89
- Lu, E.T., Hamilton, R.J., McTiernan, & J.M. Bromund, K. 1993, *ApJ*, 412, 841
- Mahadevan, R., & Quataert, E. 1997, *ApJ*, 490, 605
- McKee, C.F., & Ostriker, J.P. 1977, *ApJ*, 218, 148
- Meszáros, P. 1975, *A&A*, 44, 59
- Miller, J.S., Shahbaz, T., & Nolan, L.A. 1998, *MNRAS*, 294, 25
- Narayan, R., Quataert, E., Igumenshchev, I.V., & Abramowicz, M.A. 2002, *astro-ph/0203026*
- Oppenheimer, J., & Snyder, H. 1939, *Phys. Rev.*, 56, 455
- Paczynski, B. 1991, *ApJ*, 371, 63
- Parker, E.N. 1979, "Cosmic Magnetic Fields", Clarendon press, Oxford
- Petchek, H.E. 1963, *AAS-NASA Symp. Phys. Solar Flares*, 426
- Plokhotnichenko, V., Beskin, G., Debur, V., et al. 2003, *Nuclear Instruments and Methods in Physics A*, 513, 167
- Punsly, B. 1998a, *ApJ*, 498, 640
- Punsly, B. 1998b, *ApJ*, 498, 660
- Pustilnik, L.A., & Shvartsman, V.F. 1974, *IAUS*, 64, 213
- Pustilnik, L.A. 1977, *Soobsch. SAO*, 18, 3
- Pustilnik, L.A. 1978, *Soviet Ast.*, 22, 350
- Pustilnik, L.A. 1997, *Ap&SS*, 252, 325
- Revnivtsev, M.G., & Sunyaev, R.A. 2001, *astro-ph/0109036*
- Roberts, T.P., Goad, M.R., Ward, M.J., et al. 2002, *astro-ph/0202017*
- Ruffert, M. 1997, *A&A*, 317, 793
- Ruffert, M. 1999, *A&A*, 346, 861
- Sawada, K., Matsuda, T., Anzer, U., et al. 1989, *A&A*, 221, 263
- Shapiro, S.L. 1973a, *ApJ*, 180, 531
- Shapiro, S.L. 1973b, *ApJ*, 185, 69
- Shapiro, S.L., & Teukolsky, S.A. 1973, "Black holes, white dwarfs, and neutron stars: The physics of compact objects", New York, Wiley-Interscience
- Shapiro, S.L. 1974, *ApJ*, 189, 343
- Scharlemann, E.T. 1983, *ApJ*, 272, 279
- Shakura, N.I., & Sunyaev, R.A. 1973, *A&A*, 24, 337
- Shields, G.A. 1999, *PASP*, 111, 661
- Shvartsman, V.F. 1971, *AZh*, 48, 438.



- Shvartsman, V.F. 1977, Soobsch. SAO, 19, 3  
Shvartsman, V.F. 1989a, Afz, 31, 457  
Shvartsman, V.F. 1989b, Astron. Report Letters, 15, 337  
Spitzer, L. 1954, ApJ, 120, 1  
Stoeger, W.R. 1980, MNRAS, 190, 715  
Sunyaev, R.A. 1972, AZh, 49, 1153  
Sweet, P.A. 1969, ARA&A, 7, 149  
Srovatskii, S. I. 1981, ARA&A, 19, 163  
Will, C.M. 1998, gr-qc/9811036